NIH Public Access
Author Manuscript
Nature. Author manuscript; available in PMC 2009 August 24.

Published in final edited form as:
Nature. 2008 July 10; 454(7201): 217–220. doi:10.1038/nature07001.

An internal thermal sensor controlling temperature preference in *Drosophila*

Fumika N. Hamada[1], **Mark Rosenzweig**[1], **Kyeongjin Kang**[1], **Stefan Pulver**[1], **Alfredo Ghezzi**[1], **Timothy J. Jegla**[2], and **Paul A. Garrity**[1,‡]

[1] National Center for Behavioral Genomics, Volen Center for Complex Systems, Biology Department, Brandeis University MS-008, 415 South Street, Waltham, MA 02454

[2] Department of Biochemistry, The Scripps Research Institute, 10550 N. Torrey Pines Road, La Jolla, CA 92037

Abstract

Animals from flies to humans are able to distinguish subtle gradations in temperature and exhibit strong temperature preferences[1–4]. Animals move to environments of optimal temperature and some manipulate the temperature of their surroundings, as humans do using clothing and shelter. Despite the ubiquitous influence of environmental temperature on animal behavior, the neural circuits and strategies through which animals select a preferred temperature remain largely unknown. Here we identify a small set of warmth-activated neurons (AC neurons) located in the *Drosophila* brain whose function is critical for preferred temperature selection. AC neuron activation occurs just above the fly's preferred temperature and depends on dTRPA1, an ion channel that functions as a molecular sensor of warmth. Flies that selectively express dTRPA1 in the AC neurons select normal temperatures, while flies in which dTRPA1 function is reduced or eliminated choose warmer temperatures. This internal warmth-sensing pathway promotes avoidance of slightly elevated temperatures and acts together with a distinct pathway for cold avoidance to set the fly's preferred temperature. Thus, flies select a preferred temperature by using a thermal sensing pathway tuned to trigger avoidance of temperatures that deviate even slightly from the preferred temperature. This provides a potentially general strategy for robustly selecting a narrow temperature range optimal for survival.

Keywords

thermosensation; thermal preference; body temperature; TRP; TRPA1

While the physiology of all cells is affected by temperature, the expression of temperature-activated members of the Transient Receptor Potential (TRP) family (thermoTRPs) can make cell excitability highly temperature-responsive[5]. ThermoTRPs are cation channels with highly temperature-dependent conductances that participate in thermosensation from insects to humans[5]. The *Drosophila melanogaster* TRP channel dTRPA1 promotes larval heat avoidance [6] and can be activated by warming in ooctyes[7]. We asked whether *dTrpA1* contributes to the selection of a preferred temperature in the adult fly. When allowed to distribute along a thermal

‡To whom correspondence should be addressed. E-mail: pgarrity@brandeis.edu, Telephone: 781-736-3127; FAX: 781-736-8161.

Author contributions: F.H., M.R., S.P., K.J.K and P.G. designed experiments, F.H. performed behavior and imaging, M.R. created *dTrpA1* mutant, Gal4, RNAi and rescue strains, K.J.K performed oocyte electrophysiology and dTRPA1 overexpression, S.P. performed NMJ electrophysiology, A.G. assisted imaging, T.J.J. isolated agTRPA1 cDNA, and P.G. assisted with knockdown studies. F.H. and P.G. wrote the paper with assistance from M.R., K.J.K., S.P., and A.G.

NIH-PA Author Manuscript
NIH-PA Author Manuscript
NIH-PA Author Manuscript

NIH-PA Author Manuscript

NIH-PA Author Manuscript

NIH-PA Author Manuscript

gradient for 30 minutes, wild-type *Drosophila melanogaster* adults prefer ~25°C[3], their optimal growth temperature[8]. Compared to wild-type controls, *dTrpA1* loss-of-function mutant animals exhibited increased accumulation in the warmest (28–32°C) regions of the gradient ($P < 0.0001$), but not in the coolest (18–22°C) regions ($P=0.5$) (Fig. 1A, 1B, Supp. Fig. 1). A *dTrpA1* genomic minigene rescued the phenotype (Fig. 1A, 1B). Animals heterozygous for *dTrpA1* loss-of-function mutations also preferred slightly elevated temperatures (Supp. Fig. 2A). Thus, *dTrpA1* function is important for determining thermal preference and specifically contributes to avoidance of warm regions.

If dTRPA1 were involved in thermotransduction, dTRPA1 should regulate the warmth-responsiveness of thermosensors. As the identity of the adult *Drosophila* thermosensors was unknown, we examined dTRPA1 protein expression (using anti-dTRPA1 antisera[6]). dTRPA1 expression was detected in three sets of previously uncharacterized cells in the brain: LC (lateral cell), VC (ventral cell), and AC (anterior cell) neurons (Fig. 2A). (dTRPA1 was also detected in the proboscis, but ablation studies detected no contribution of the proboscis to warmth avoidance (Supp. Fig. 3).) To focus on neurons most likely to contribute to thermal preference, we examined where the rescuing *dTrpA1* minigene restored dTRPA1 expression. The minigene restored dTRPA1 expression specifically within AC neurons, but not LC or VC (Fig. 2B). This suggested dTRPA1 expression in AC neurons, two pairs of neurons at the brain's anterior, sufficed to restore thermal preference, and that AC's might be thermosensors.

Temperature-responsiveness of AC neurons was examined using the calcium indicator G-CaMP[9] (Fig. 2A, 2C). When exposed to increasing temperature, AC neurons exhibited robust increases in G-CaMP fluorescence, reflecting warmth-responsive increases in intracellular calcium (Fig. 2H, 2I and 2K). 10 of 27 AC neurons imaged had fluorescence increases between 4% and 39%, with a mean increase over baseline ($\Delta F/F$) among these cells of 15% (+/− 4% SEM, n=10)(Fig. 2M). The mean temperature at which fluorescence increases were initially observed was 24.9°C (+/−0.6, n=10), compatible with AC activation as temperatures rise above preferred. In contrast, no *dTrpA1* mutant AC neurons imaged exhibited fluorescence increases (n=21) (Fig. 2J, 2L, 2M) ($P<0.003$ compared with wild type, Fisher's exact test). As a control that mutant AC neurons remained physiologically active, we confirmed that they showed robust $\Delta F/F$ responses upon KCl addition (Supp. Fig. 4). Importantly, AC responses did not depend on an intact periphery, as all G-CaMP studies were performed using isolated brains from which peripheral tissues had been removed. These observations identify AC neurons as warmth-activated, dTRPA1-dependent thermosensors.

AC neurons project toward several brain regions, including the Antennal Lobe (AL) (Fig. 2D-2G). The AL is implicated in cockroach thermosensation[10], but has been studied exclusively for olfaction in *Drosophila*. To date, 11 of the ~50 AL glomeruli remain unassociated with identified olfactory receptors[11]. AC neurites elaborated within two such "mystery" glomeruli, VL2a and VL2p (Fig. 2E). Thus the *Drosophila* AL receives both thermosensory and olfactory neuron innervation. VL2a is also innervated by Fruitless-expressing neurons implicated in pheromone transduction[11], suggesting that even individual glomeruli receive multi-modal sensory information. AC processes also branched within the Subesophageal Ganglion (SOG) and Superior Lateral Protocerebrum (SLRP), although these target regions are less defined than in the AL. The SOG and SLRP have been previously implicated in processing olfactory and gustatory input[12].

As dTRPA1 expression in AC neurons appeared sufficient to restore normal thermal preference, we examined whether it was also necessary. dTRPA1 was knocked down selectively in AC neurons using tissue-specific anti-dTRPA1 RNAi controlled by *dTrpA1^{SH}-Gal4* (Fig. 3A), a promoter expressed in AC but not LC or VC neurons. Consistent with the importance of dTRPA1 expression in AC neurons in thermal preference, AC-knockdown

NIH-PA Author Manuscript

NIH-PA Author Manuscript

NIH-PA Author Manuscript

increased the fraction of animals present in the 28–32°C region compared to controls (P≤0.0001) (Fig. 3B, 3C). Similar results were obtained when dTRPA1 expression was knocked down using a broad neuronal promoter (*Appl-Gal4*) (Fig. 3C, Supp. Fig. 2B). (All knockdowns were assessed with dTRPA1 immunohistochemistry.) dTRPA1 knockdown with the general cholinergic neuron promoter *Cha(7.4)-Gal4* eliminated detectable dTRPA1 expression in AC neurons (and in VC and LC) and decreased warmth avoidance (Fig. 3C, Supp. Fig. 2C). In contrast, dTRPA1 RNAi expressed using *Cha(1.2)-Gal4* (which is expressed in many brain cholinergic neurons[13], but not the AC's) did not disrupt warmth avoidance (Fig. 3C, Supp. Fig. 2D). Taken together, our data suggest dTRPA1 expression in AC neurons (but not LC or VC) is both necessary and sufficient for normal thermal preference behavior. Whether LC and VC neurons participate in other warmth-activated responses is unknown.

The identification of an internal sensor controlling temperature preference conflicts with the established view that *Drosophila* sense moderate warming using thermosensors in the third antennal segment[3]. We re-examined the effects of surgically removing either one third antennal segment and arista (unilateral ablation) or both (bilateral ablation). In our hands (see methods), both unilateral and bilateral ablation increased the fraction of animals in cool (18–22°C), but not warm (28–32°C) regions (Fig. 3D, 3F). Thus these tissues were dispensable for warmth avoidance, but essential for cool avoidance. When *dTrpA1* mutants were subjected to bilateral ablation, such "*dTrpA1* ab" animals accumulated in both cool and warm regions (Fig. 3E): the fraction between 18–22°C did not differ from wild-type ablation animals (P=1.0), and the fraction between 28–32°C did not differ from non-ablated *dTrpA1* mutants (P=0.9) (Fig. 3F). Thus dTRPA1-expressing cells and antennal cells function additively to set preferred temperature, promoting avoidance of elevated and reduced temperatures, respectively.

These data are consistent with warmth activation of dTRPA1 serving as the molecular basis for AC neuron function. As thermal activation of mammalian TRPA1 proteins is controversial, we tested whether dTRPA1 could act as a molecular sensor of warming in the fly. Indeed, mis-expression of dTRPA1 throughout the fly nervous system (using *c155-Gal4*) caused a dramatic phenotype not observed in controls: heating these flies to 35°C for 60 seconds caused incapacitation, an effect reversed upon return to 23°C (Fig. 4A, Supp. Movie 1). Similar effects were observed using electrophysiology, with moderate warming (above ~25°C) triggering a barrage of excitatory junction potentials (EJP's) at the neuromuscular junction (Fig. 4B, 4C, Supp. Fig. 5). These data strongly support dTRPA1 acting as a molecular sensor of warming. The ability of dTRPA1 mis-expression to confer warmth-activation also suggests dTRPA1 can be used as a genetically encoded tool for cell-specific, inducible neuronal activation. dTRPA1 might be particularly useful in tissues like the fly brain where thermal stimulation is easier to deliver than the chemical or optical stimulation that controls other tools for modulating neuronal activity.

To test whether warmth activation is a property of other insect TRPA1s, we examined the malaria mosquito *Anopheles gambiae* TRPA1 (agTRPA1). As previously reported, dTRPA1 is warmth-activated when expressed in *Xenopus laevis* oocytes (Fig. 4D, 4F). We found agTRPA1 also exhibited robust warmth activation (Fig. 4E, 4G). These currents were specific; they were not observed in uninjected oocytes (Supp. Fig. 6) and were inhibited by Ruthenium Red (which antagonizes other TRPs). Like mammalian thermoTRPs, both dTRPA1 and agTRPA1 exhibited outward rectification (Fig. 4F, 4G). Closely related TRPA1s are present in the flour beetle *Tribolium* and in disease vectors like *Pediculus humanus corporis* (body lice), *Culex pipiens* (common house mosquito), and *Anopheles aedes* (yellow and dengue fever mosquito) which use warmth-sensing for host location and habitat selection[14, 15] (Supp. Fig. 7). Such insect TRPA1s constitute potential targets for disrupting thermal preference and other thermosensory behaviors in agricultural pests and disease vectors.

NIH-PA Author Manuscript

NIH-PA Author Manuscript

NIH-PA Author Manuscript

While previously identified ambient thermoreceptors are peripheral[4, 16–19], AC neurons are internal. As an ~1 mg fly is readily penetrated by ambient temperature variations[20, 21], such an internal sensor should monitor environmental temperature effectively. Internal thermosensors like the hypothalamus (which regulates body temperature) are well-established in mammals[22]. In insects, thermoregulatory studies have long implied the existence of internal thermoreceptors[21], but the AC neurons are the first described at the cellular level. The AC's become active as temperatures rise above preferred, suggesting they may function as "discomfort" receptors that, together with putative antennal cool receptors (like those found in other insect antennae[18]), repel the fly from all but the most optimal temperatures. Related strategies may act in mammals: mice lacking the cool-activated channel TRPM8 prefer abnormally cool temperatures, while mice lacking the heat-activated channel TRPV4 prefer warmer temperatures[22].

Environmental temperature affects the physiology of all animals. Increasing temperatures associated with climate change have been linked to pole-ward redistributions of hundreds of species including insects, fish, birds and mammals [23]. Understanding how animals detect and respond to environmental temperature variation is critical for understanding how organisms survive in and adapt to a dynamic climate.

Methods Summary

Fly strains and Immunohistochemistry

The *dTrpA1* rescue transgene contains an NheI-XhoI genomic fragment (from 2.5 kb upstream to 1.2 kb downstream of the dTRPA1 open reading frame) in pPelican containing Su(Hw) insulators [24]. *dTrpA1^{SH}-Gal4* contains a Gal4 coding region flanked 5′ by 2.5 kb upstream of dTRPA1 start codon and 3′ by 1.7 kb of *dTrpA1* sequences from exon 1 to the fourth intron and inserted into pPelican. *dTrpA1^{SH}-Gal4* differs from the previously described *dTrpA1-Gal4*6, and the two drivers overlap distinct subsets of dTRPA1-expressing cells. *dTrpA1^{ins}* was generated by ends-in gene targeting[25] and contains a tandem array of two mutated copies of *dTrpA1* as shown in Supp. Fig. 1. One copy is deleted for the sixth transmembrane domain and C-terminus, while the other copy is deleted for the promoter region and start codon and contains a translational stop prior to the transmembrane domains. *Df(3L)ED4415* is a chromosomal deficiency that completely removes the *dTrpA1* locus. dTRPA1 RNAi constructs were designed using the strategy of Kalidas and Smith [26] and generated as described [27]. Additional details are provided in Methods section.

Temperature preference behavior—Temperature preference behavior assay was modified from Sayeed et al. [3] as detailed in Methods section.

Physiology—For G-CaMP imaging, brains from live *dTrpA1^{SH}-Gal4;UAS-G-CaMP* (WT) or *dTrpA1^{SH}-Gal4;UAS-G-CaMP;dTRPA1^{ins}* flies were dissected in Modified Standard Solution F (5 mM Na-HEPES, 115 mM NaCl, 5 mM KCl, 6 mM $CaCl_2$, 1 mM $MgCl_2$, 4 mM $NaHCO_3$, 5 mM trehalose, 10 mM glucose, 65 mM sucrose, pH 7.5) [28] by removing the cuticule from the head and trachea using fine forceps. The brain was severed from the body and placed onto Sylgard-coated coverslips, anterior side facing up. Brains were imaged as detailed in Methods section. Oocyte physiology and larval recordings were performed as detailed in Methods section.

NIH-PA Author Manuscript

NIH-PA Author Manuscript

NIH-PA Author Manuscript

Methods

Fly strains

The *dTrpA1* rescue transgene contains an NheI-XhoI genomic sequence fragment (extending from 2.5 kb upstream of the dTRPA1 start codon to 1.2 kb downstream of the stop codon) inserted into a pPelican vector containing Su(Hw) insulator sequences [24]. *dTrpA1^{SH}-Gal4* contains a Gal4 coding region flanked 5′ by 2.5 kb upstream of the dTRPA1 start codon and 3′ by 1.7 kb of *dTrpA1* sequences from exon 1 to the fourth intron and inserted into pPelican. Please note that *dTrpA1^{SH}-Gal4* differs from the previously described *dTrpA1-Gal4*6 as it contains more *dTrpA1* sequences as well as flanking Su(Hw) insulator sequences, and the two drivers overlap distinct subsets of dTRPA1-expressing cells. The *dTrpA1^{ins}* mutant was generated by ends-in homologous recombination-mediated gene targeting[25] and contains a tandem array of two mutated copies of *dTrpA1*: one copy lacks DNA encoding the predicted sixth transmembrane domain and the C-terminus, while the other copy lacks DNA sequences containing the putative promoter region and predicted start codon and carries an insertion creating a translational stop prior to the transmembrane domains. The targeting construct was generated by cloning a BglI-KpnI dTRPA1 genomic DNA fragment from BAC RP98-10P9 (Open Biosystems) into pBluescriptII. An I-SceI site was inserted into the BamHI site in exon 8 of dTRPA1 and a ClaI site in exon 4 was filled in to generate the engineered frameshift mutation), and the construct was cloned into NotI/KpnI digested pTV2 for targeting as described[25]. The organization of the *dTrpA1^{ins}* mutant locus is described in Supplementary Fig. 1. *Df(3L)4415* is a chromosomal deficiency that completely removes the *dTrpA1* locus. dTRPA1 RNAi constructs were designed using the strategy of Kalidas and Smith [26] and generated as described [27]. *UAS-dTRPA1^{RNAi}* flies contain two copies each of *UAS-dTRPA1^{RNAi}-A* and *UAS-dTRPA1^{RNAI}-B*. PCR primers used to create UAS-dTRPA1^{RNAi}-A were: genomic fragment 5′-ATAACTGAGTTCGATGCATGCCCACG and 5′-GCCTCGAGACTAGTCTGGAAAAATGGAAAGCCAAGT; cDNA fragment 5′-GCTCTAGAATAACTGAGTTCGATGCATGCCCACG and 5′-CACTCGAGACTAGTCTGTTTTCCAACCGCTACGAG. PCR primers used to create UAS-dTRPA1^{RNAi}-B were: genomic fragment 5′-AGGAGCGGGCCAACGAGGTGATG and 5′-GCCTCGAGACTAGTCTGAAAAATGGAGGTGTTGCTATATG; cDNA fragment 5′-ATTCTAGAAGGAGCGGGCCAACGAGGTGATG and 5′-GCCTCGAGACTAGTCCCATATTGCAGTATTGACTCATC. Additional fly strains were obtained from Bloomington, except for *Cha(7.4)-Gal4* and *Cha(1.2)-Gal4* from P. Salvaterra, *Appl-Gal4* from T. Tayler, *Dll-Gal4* from G. Boekh, *UAS-G-CaMP* from R. Axel.

Temperature preference behavior—Temperature preference behavior assay was designed according to Sayeed et al. [3], but with a larger temperature range. Air temperatures inside the apparatus were determined using a Fluke 52II thermometer with multiple temperature probes. The apparatus was coated with Rain-X to prevent flies from escaping the temperature gradient. Rain-X does not disturb the normal temperature preference (data not shown). For each assay, ~20–30 adult flies (0–3 days old) were blown into the apparatus through a hole at the midpoint of the gradient and exposed to the gradient for 30 min in darkness prior to data collection. All experiments were performed in an environmental room maintained at 25 °C/70%RH.

We plot performance as a function of the air temperature within the behavioral chamber. We monitored both air and apparatus surface temperatures, but found that relying on air temperature significantly decreased variation in behavior between experiments, suggesting this parameter was more relevant to the fly (FH and PG, unpublished). As the surface temperature gradient is steeper than the air temperature gradient (FH and PG, unpublished), our thermal gradients extended to both warmer and cooler temperatures than the Sayeed and Benzer

NIH-PA Author Manuscript

NIH-PA Author Manuscript

NIH-PA Author Manuscript

gradients (~31.5°C in surface temperature is ~29°C in air temperature). Our finding that adults lacking third antennal segments avoid warm regions of the thermal gradient was initially unexpected, as Sayeed and Benzer reported that removal of the third antennal segment eliminated temperature preference [3]. However, these authors did note that the distribution of ablated flies fell off significantly at higher temperatures, approaching zero near 31.5°C. The apparent differences in our results may reflect, in part, subtle differences in assay environment including the monitoring of only surface temperature in the previous study [3]. Irrespective of subtle differences in our data sets, our ablation data together with our *dTrpA1* mutant analysis clearly demonstrate that avoidance of warm temperatures persists in the absence of the third antennal segment. Our conclusion that unilateral ablation causes a partial decrease in cold avoidance also differs from the stated conclusion of Sayeed and Benzer that such an ablation had no effect [3]. However, their published data show that they also observed a significant (>3-fold) increase in the fraction of flies in the 18–22.5°C region (from ~15% to ~50%).

Immunostaining—Immunostaining was performed as described [6] except 5% normal goat serum and 1% BSA in PBST (1% Triton X-100) were used for blocking and antibody incubations. PBST (1% Triton X-100) were used for washing. Antibodies used were: rat anti-dTRPA1 [6], at 1:1000; rabbit anti-RFP (Chemicon), at 1:200; mouse nc82 (Developmental Studies Hybridoma Bank), at 1:40;goat anti-rat Cy3 (Jackson ImmunoResearch), at 1:4000; goat anti-rat Cy5 (Jackson ImmunoResearch), at 1:200; goat anti-rabbit Cy3 (Jackson ImmunoResearch) at 1:200; goat anti-mouse Cy5 (Jackson ImmunoResearch) at 1:200.

Calcium imaging: fly preparation and imaging—Brains from live *dTrpA1^{SH}-Gal4;UAS-G-CaMP* (WT) and *dTrpA1^{SH}-Gal4;UAS-G-CaMP;dTRPA1^{ins}* flies were dissected in Modified Standard Solution F (5 mM Na-HEPES, 115 mM NaCl, 5 mM KCl, 6 mM $CaCl_2$, 1 mM $MgCl_2$, 4 mM $NaHCO_3$, 5 mM trehalose, 10 mM glucose, 65 mM sucrose, pH 7.5) [28] by removing the cuticle from the head and trachea using fine forceps. The brain was severed from the body and placed onto Sylgard-coated coverslips, anterior side facing up. The brain was then glued to the slide by applying small amounts of Vetbond™ (3M) between the external edge of the optic lobes and the slide using a pulled glass capillary. The slide was mounted on a laminar flow perfusion chamber (~500 µl volume) beneath a 40X or 60X water immersion objective of a fixed stage upright microscope (Olympus BX51W1), illuminated using a 75W xenon Apo lamp with a 490 nm excitation filter and visualized through a 528 emission filter (Olympus). During experiments, the preparation was constantly perfused with Modified Standard Solution F via gravity flow at a rate of ~3 ml/min. The solution temperature was gradually increased from room temperature (~22°C) to 33° C using a CL-100 Bipolar Temperature Controller equipped with a SC-20 Dual In-line Solution Heater/Cooler (Warner Instruments). Optical images of the preparation were acquired during the temperature shift using a digital CCD camera (Hamamatsu C4742-80-12AG) at 4 frames per second with 512 × 512 pixel resolution. The image data was digitized and analyzed using Volocity software (Improvision). For analysis, areas representing G-CaMP expressing cell bodies were circumscribed and the mean fluorescent intensity was calculated for each region of interest at every frame. Background fluorescence (calculated from the average fluorescence of two randomly chosen non-G-CaMP expressing areas) was subtracted from the mean fluorescent intensity of the regions of interest. Background-subtracted values were then expressed as % ΔF/F, where F is the mean fluorescence intensity in the 10 seconds prior to stimulation. The solution temperature was simultaneously recorded and digitized using PowerLab 4/30 and Chart software (AD Instruments) and synchronized with the image acquisition through an Orbit II Controller (Improvision). Bleaching corrections were done by plotting a least-squares fit line in Excel using the first 10 seconds of imaging and extrapolating this bleaching rate for the duration of the experiment. Pseudo-color images were generated in Adobe Photoshop from

NIH-PA Author Manuscript

NIH-PA Author Manuscript

NIH-PA Author Manuscript

pixel grayscale values by setting black level values to 40 and converting to pseudo-color using the Spectrum tool.

Oocyte electrophysiology—Oocyte-positive *Xenopus laevis* females were obtained from Nasco (Ft. Atkinson, WI), and maintained at ~19°C with 12h/12h dark/light cycles. Ovaries were surgically isolated, and treated with 1.5 mg/ml of collagenase type II (Worthington, Lakewood, NJ) for 90 min, and individual oocytes were defolliculated with a pair of forceps. cRNA was transcribed by mMessage mMachine T3 kit (Ambion, Austin, TX) from each cDNA construct, and 50 nl aliquot per oocyte was injected using an automatic Drummond microinjector. (agTRPA1 sequence deposited as Genbank #1081610**.)** Membrane potential was maintained at −60 mV by two electrode voltage clamping (TEVC) during warm-activated current recording. Resistance of pulled glass capillary electrodes filled with 3 M KCl was between 0.5 and 1.5 MΩ. Typical resting membrane potentials of oocytes used for current recording were between −25 and −60 mV. Current was recorded at 2 kHz and filtered to 1 kHz with the output filter of the amplifier (OC-725B, Warner instruments, Hamden, CT). Temperature of the oocyte perfusion buffer (96 mM NaCl, 1 mM $MgCl_2$, 4 mM KCl, and 5 mM HEPES, pH 7.6) was changed by SC-20 in-line heater/cooler (Warner Instruments) under the control of CL-100 Bipolar Temperature Controller (Warner Instruments). Where indicated 50 nl of 20 mM BAPTA was injected to oocytes 30 min before recording to minimize elevations in cytosolic Ca^{++} concentration. pClamp 8.0 and Sigmaplot 8.0 were used in order to acquire and analyze the data. Voltage steps (−140 mV to 100 mV) were applied to assess I-V relationship of dTRPA1- or AgTRPA1-expressing oocytes. Each voltage step lasted 100 ms following 10 ms holding at −60 mV, and the recorded current in the last 40 ms was averaged to determine the current amplitude at a given voltage.

Larval Electrophysiology—All larval dissections and physiological recordings were performed in HL3.1 physiological saline containing (in mM) 70 NaCl, 5 KCl, 0.8 $CaCl_2$, 4 $MgCl_2$, 10 $NaHCO_3$, 5 trehalose, 115 sucrose, 5 HEPES, pH 7.1–7.2, osmolarity was ~309 mmol/kg.

Female third instar larvae were first filleted and pinned dorsal side up in a Sylgard lined Petri dish (Dow Corning, Midland, MI). The gut and trachea were removed with fine forceps, exposing the larval body wall muscles. The anterior lobes of the larval brain were removed, but the rest of the ventral ganglion was left undisturbed, preserving the cell bodies of motor neurons innervating body wall muscles.

Larval preparations were mounted on the stage of a BX50WI compound microscope (Olympus, Center Valley, PA) and continuously superfused with HL3.1 using a custom built gravity fed perfusion system. Temperature ramps were performed by circulating hot, then cold water past coils of perfusion tubing sealed in a PVC pipe on the way to the prep. Bath temperature was ramped from 23°C to 29°C then back to 23°C in every experiment. Ramp time was typically 3–5 minutes each way. Bath temperatures were monitored with a Physitemp (Clifton, NJ) model BAT-12 thermometer with thermocouple probe or alternatively using an SC-20 in-line heater/cooler (Warner Instruments) under the control of CL-100 Bipolar Temperature Controller (Warner Instruments).

Larval muscle 6 was targeted for intracellular work. EJP frequency in m6 was monitored in control and experimental animals as bath temperatures rose and fell. Recordings from m6 were performed with sharp glass electrodes (12–18 Mohms) filled with 3 M KCl. Voltage signals were amplified with either an Axoclamp 2A or Axopatch 200B (Axon Instruments, Foster City, CA) and digitized with a Powerlab 4/30 data acquisition system (ADinstruments, Colorado Springs, Co). Voltage traces were recorded in Chart 5.1 (ADinstruments). The data were

NIH-PA Author Manuscript

NIH-PA Author Manuscript

NIH-PA Author Manuscript

analyzed using scripts in Spike 2 (version 5, CED, Cambridge, UK) and standard features in Microsoft Excel (Redmond, WA).

Supplementary Material

Refer to Web version on PubMed Central for supplementary material.

Acknowledgments

We thank Garrity lab members and L. Griffith, L. Huang, R. Huey, E. Marder, M. Rosbash, P. Sengupta, G. Turrigiano and their laboratories for advice and manuscript comments. Supported by NINDS (PO1 NS044232, P30 NS045713S10 and RR16780), NEI (RO1 EY13874, P.A.G.), NIMH (RO1 MH067284, to L. Griffith [for S.P. and A.G.]), and Japan Society for the Promotion of Science (F.N.H.)

References

1. Fraenkel, G.; Gunn, D. The Orientation of Animals. Kineses, Taxes and Compass Relations. Clarendon Press; Oxford: 1940.
2. Fanger PO, Ostberg O, Nicholl A, Breum NO, Jerking E. Thermal comfort conditions during day and night. European Journal of Applied Physiology 1974;33:255–263.
3. Sayeed O, Benzer S. Behavioral genetics of thermosensation and hygrosensation in Drosophila. Proc Natl Acad Sci U S A 1996;93:6079–6084. [PubMed: 8650222]
4. Mori I. Genetics of chemotaxis and thermotaxis in the nematode Caenorhabditis elegans. Annu Rev Genet 1999;33:399–422. [PubMed: 10690413]
5. Dhaka A, Viswanath V, Patapoutian A. TRP Ion Channels and Temperature Sensation. Annu Rev Neurosci 2006;29:135–161. [PubMed: 16776582]
6. Rosenzweig M, et al. The Drosophila ortholog of vertebrate TRPA1 regulates thermotaxis. Genes Dev 2005;19:419–424. [PubMed: 15681611]
7. Viswanath V, et al. Opposite thermosensor in fruitfly and mouse. Nature 2003;423:822–823. [PubMed: 12815418]
8. Siddiqui WH, Barlow CA. Population growth of Drosophila melanogaster (Dipetera:Drosophilidae) at constant and alternating temperatures. Ann Entomol Soc Amer 1972;65:993–1001.
9. Nakai J, Ohkura M, Imoto K. A high signal-to-noise Ca(2+) probe composed of a single green fluorescent protein. Nat Biotechnol 2001;19:137–141. [PubMed: 11175727]
10. Fischer H, Tichy H. Cold-receptor cells supply both cold- and warm-responsive projection neurons in the antennal lobe of the cockroach. J Comp Physiol A Neuroethol Sens Neural Behav Physiol 2002;188:643–648. [PubMed: 12355240]
11. Vosshall LB, Stocker RF. Molecular architecture of smell and taste in Drosophila. Annu Rev Neurosci 2007;30:505–533. [PubMed: 17506643]
12. Ito K, et al. The organization of extrinsic neurons and their implications in the functional roles of the mushroom bodies in Drosophila melanogaster Meigen. Learn Mem 1998;5:52–77. [PubMed: 10454372]
13. Kitamoto T, Ikeda K, Salvaterra PM. Regulation of choline acetyltransferase/lacZ fusion gene expression in putative cholinergic neurons of Drosophila melanogaster. J Neurobiol 1995;28:70–81. [PubMed: 8586966]
14. Brown AWA. Factors in the attractives of bodies for mosquitoes. Nature 1951;167:202. [PubMed: 14806426]
15. Friend WG, Smith JJB. Factors affecting feeding by bloodsucking insects. Ann Rev Entomol 1977;22:309–331. [PubMed: 319741]
16. Patapoutian A, Peier AM, Story GM, Viswanath V. ThermoTRP channels and beyond: mechanisms of temperature sensation. Nat Rev Neurosci 2003;4:529–539. [PubMed: 12838328]
17. Tominaga M, Caterina MJ. Thermosensation and pain. J Neurobiol 2004;61:3–12. [PubMed: 15362149]

NIH-PA Author Manuscript

NIH-PA Author Manuscript

NIH-PA Author Manuscript

18. Tichy, H.; Gingl, E. Problems in hygro- and thermoreception. In: Barth, FG.; Schimd, A., editors. The ecology of sensing. Springer; New York: 2001. p. 271-287.

19. Liu L, Yermolaieva O, Johnson WA, Abboud FM, Welsh MJ. Identification and function of thermosensory neurons in Drosophila larvae. Nat Neurosci 2003;6:267–273. [PubMed: 12563263]

20. Stevenson RD. Body size and limits to the daily range of body temperature in terrestrial ectotherms. American Naturalist 1985;125:102–117.

21. Heinrich, B. The Hot-Blooded Insects: Strategies and Mechanisms of Thermoregulation. Harvard University Press; 1993.

22. Caterina MJ. Transient receptor potential ion channels as participants in thermosensation and thermoregulation. American journal of physiology 2007;292:R64–76. [PubMed: 16973931]

23. Parmesan C, Yohe G. A globally coherent fingerprint of climate change impacts across natural systems. Nature 2003;421:37–42. [PubMed: 12511946]

24. Barolo S, Castro B, Posakony JW. New Drosophila transgenic reporters: insulated P-element vectors expressing fast-maturing RFP. BioTechniques 2004;36:436–440. 442. [PubMed: 15038159]

25. Rong YS, Golic KG. Gene targeting by homologous recombination in Drosophila. Science 2000;288:2013–2018. [PubMed: 10856208]

26. Kalidas S, Smith DP. Novel genomic cDNA hybrids produce effective RNA interference in adult Drosophila. Neuron 2002;33:177–184. [PubMed: 11804566]

27. Tayler TD, Robichaux MB, Garrity PA. Compartmentalization of visual centers in the Drosophila brain requires Slit and Robo proteins. Development 2004;131:5935–5945. [PubMed: 15525663]

28. Ng M, et al. Transmission of olfactory information between three populations of neurons in the antennal lobe of the fly. Neuron 2002;36:463–474. [PubMed: 12408848]

NIH-PA Author Manuscript

NIH-PA Author Manuscript

NIH-PA Author Manuscript

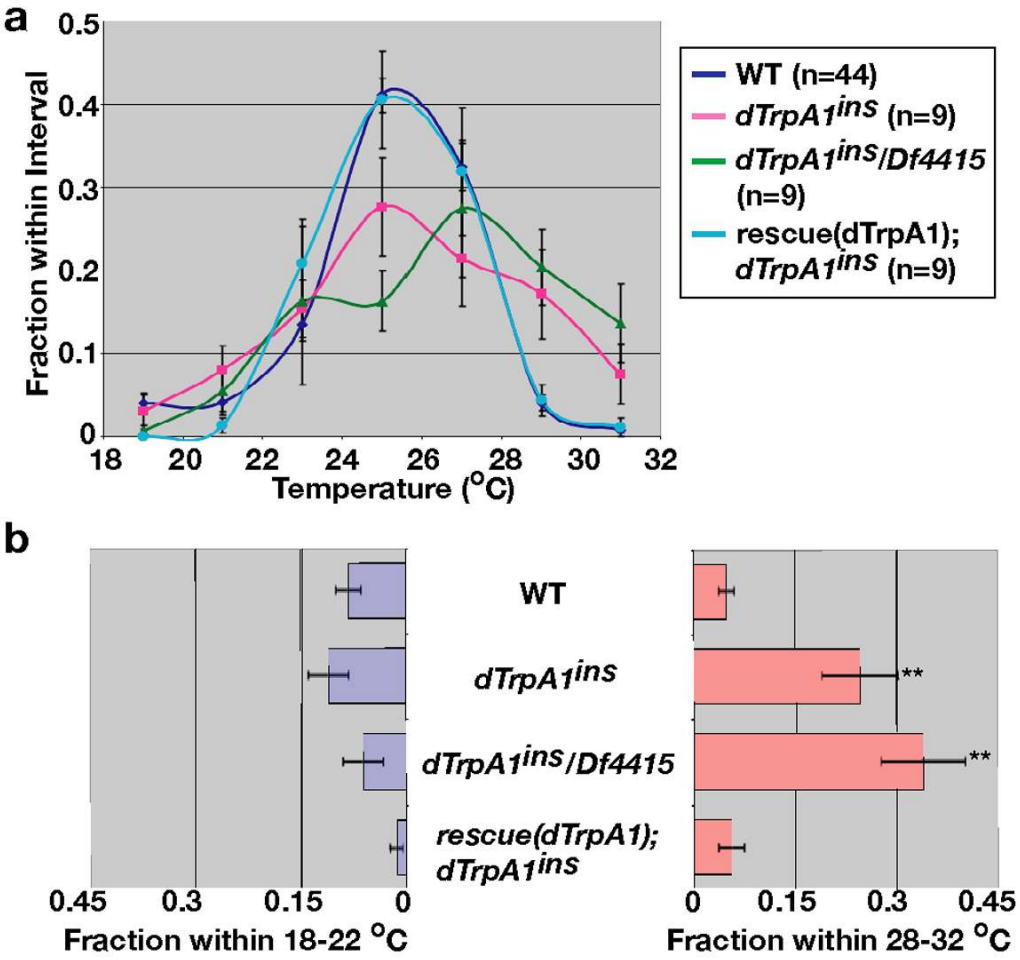

Figure 1. *dTrpA1* is required for warmth avoidance

a, Distribution of animals on thermal gradient. **b,** Fraction of animals in 18–22°C (blue) and 28–32°C (red) regions of thermal gradient. Data are mean +/− SEM. n= number of assays. ** P≤0.0001 compared to wild type (unpaired t-test).

NIH-PA Author Manuscript
NIH-PA Author Manuscript
NIH-PA Author Manuscript

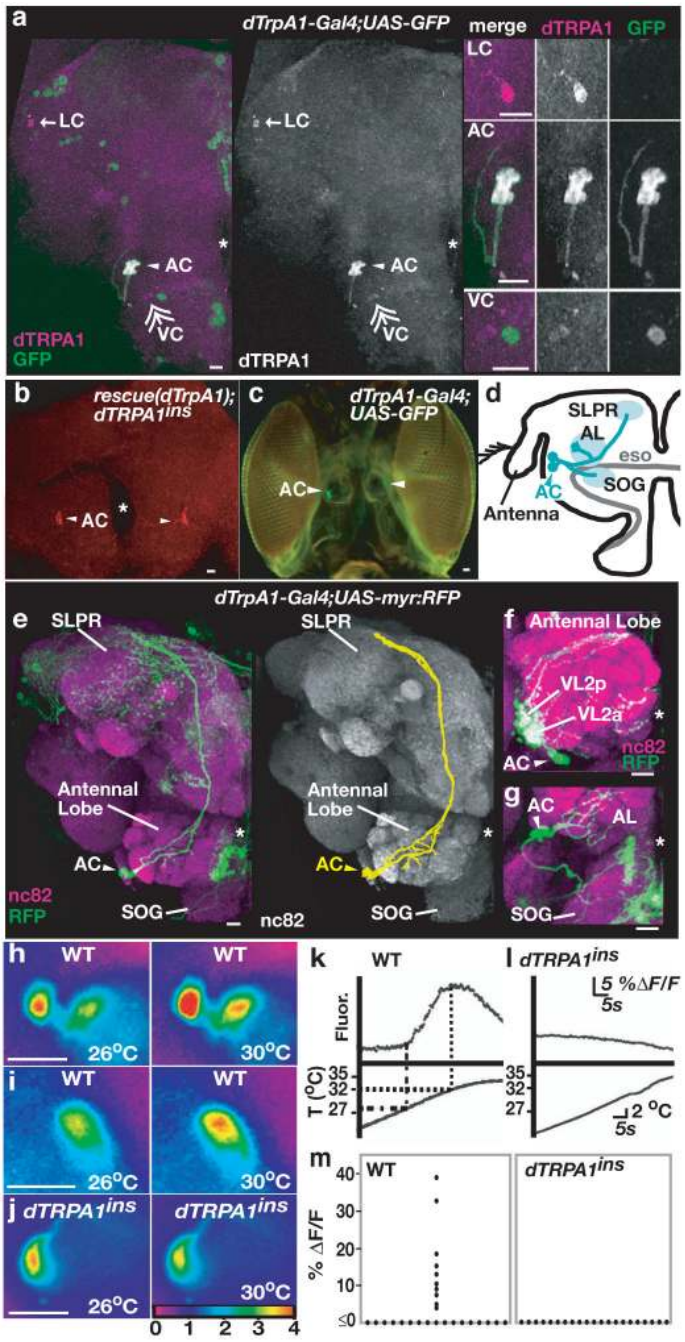

Figure 2. AC neurons are thermosensors

a, AC (arrowhead), LC (arrow) and VC (double arrow) neurons. **b,** dTRPA1 minigene expression. **c,** AC locations (antennae removed). **d,** AC projections. **e,** Left, AC processes labeled using *dTrpA1^{SH}-Gal4;UAS-myr:RFP*. Also labeled are cells that express *dTrpA1^{SH}-Gal4*, but do not detectably express dTRPA1 protein [also see **a**]. Right, camera-lucida-style outline of AC projections. **f–g,** AC projections to AL (**f**) and SOG (**g**). **h–j,** G-CaMP-labeled AC's. Two AC's sometimes imaged simultaneously (**h**). **k–l,** Warmth-responsive G-CaMP fluorescence of AC's. **m,** Maximum F/F each AC imaged. AL, antennal lobe; SOG, subesophageal ganglion; SLPR, superior lateral protocerebrum; eso (asterisk), esophagus.

NIH-PA Author Manuscript
NIH-PA Author Manuscript
NIH-PA Author Manuscript

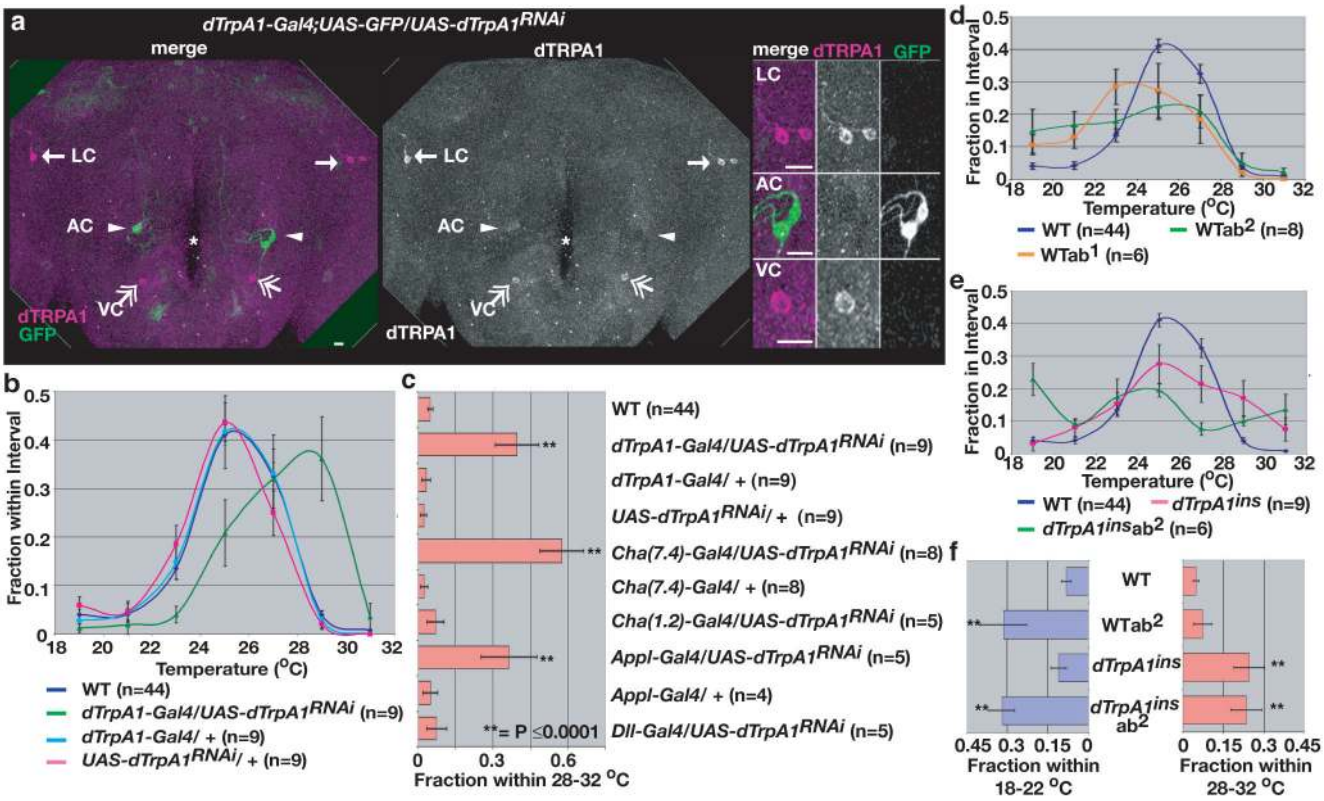

Figure 3. AC neurons are necessary for warmth avoidance

a, AC-specific knockdown of dTRPA1 protein expression in *dTrpA1* ^{SH}*-Gal4;UAS-GFP;UAS-dTrpA1* ^{RNAi} animals: dTRPA1 is expressed in LC (arrow) and VC (double arrow), but not AC neurons (arrowhead). GFP marks dsRNA-expressing cells. Two left panels show adult brain and right hand panels show close-ups of specific cells. **b,** Distribution of indicated genotypes along thermal gradient. **c,** Fraction of RNAi animals in 28–32°C region of gradient. **d,e,** Animal distributions along thermal gradient. ab^1, unilateral ablation. ab^2, bilateral ablation. **f,** Fraction of animals in 18–22°C (blue) and 28–32°C (red) regions of gradient.

NIH-PA Author Manuscript

NIH-PA Author Manuscript

NIH-PA Author Manuscript

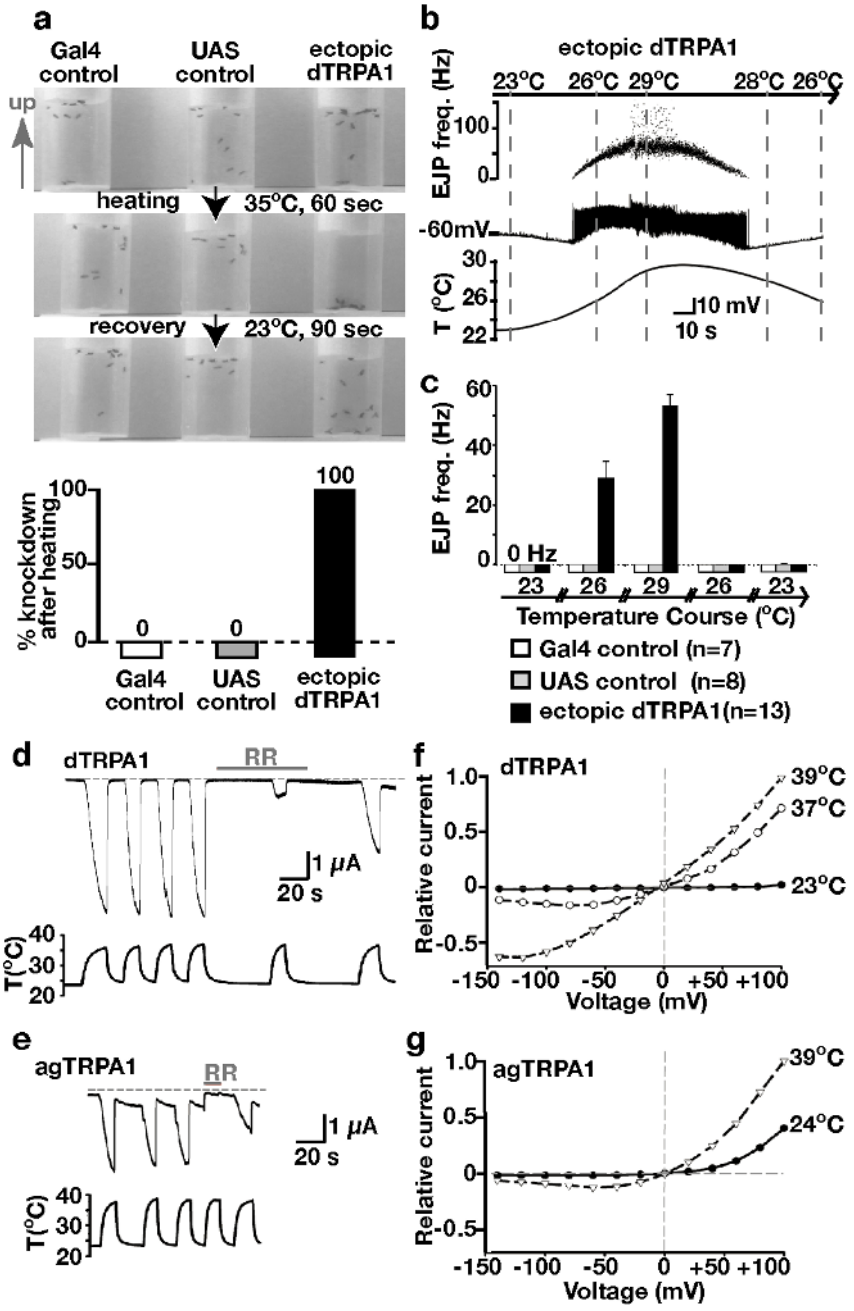

Figure 4. dTRPA1 is a warmth sensor

a, Flies expressing dTRPA1 in all neurons (*c155-Gal4;UAS-dTRPA1*) are incapacitated after 60 sec at 35°C, but recover at 23°C. Gal4 control, *c155-Gal4*. UAS control, *UAS-dTRPA1*. Ectopic dTRPA1, *c155-Gal4;UAS-dTRPA1*. Five experiments/genotype, 15 flies/experiment, SEM's=0. **b, c.** Warming (above ~25°C) stimulates transmission at neuromuscular junction in *c155-Gal4;UAS-dTRPA1*. **d–g,** dTRPA1 and agTRPA1 are warmth-activated in oocytes (n>14 each). **d,e** Warmth-evoked currents in dTRPA1 or agTRPA1-expressing oocytes (−60mV). Oocytes were injected with BAPTA 30 min prior to recording, minimizing cytosolic Calcium elevations. RR: 50 micromolar Ruthenium Red. **f,g** Current-voltage relationships of dTRPA1 and agTRPA1 at indicated temperatures.